JOURNAL OF THE ROYAL SOCIETY Interface

J. R. Soc. Interface (2012) **9**, 1856–1868
doi:10.1098/rsif.2012.0084
Published online 22 February 2012

Fish and robots swimming together: attraction towards the robot demands biomimetic locomotion

Stefano Marras[1,2] and Maurizio Porfiri[1,*]

[1]*Department of Mechanical and Aerospace Engineering, Polytechnic Institute of New York University, Six MetroTech Center, 11201 Brooklyn, NY, USA*
[2]*IAMC–CNR, Località Sa Mardini, Torregrande, 09072 Oristano, Italy*

The integration of biomimetic robots in a fish school may enable a better understanding of collective behaviour, offering a new experimental method to test group feedback in response to behavioural modulations of its 'engineered' member. Here, we analyse a robotic fish and individual golden shiners (*Notemigonus crysoleucas*) swimming together in a water tunnel at different flow velocities. We determine the positional preference of fish with respect to the robot, and we study the flow structure using a digital particle image velocimetry system. We find that biomimetic locomotion is a determinant of fish preference as fish are more attracted towards the robot when its tail is beating rather than when it is statically immersed in the water as a 'dummy'. At specific conditions, the fish hold station behind the robot, which may be due to the hydrodynamic advantage obtained by swimming in the robot's wake. This work makes a compelling case for the need of biomimetic locomotion in promoting robot–animal interactions and it strengthens the hypothesis that biomimetic robots can be used to study and modulate collective animal behaviour.

Keywords: biomimetics; collective behaviour; fish swimming; hydrodynamics; leadership; robotics

1. INTRODUCTION

Fish schooling has always attracted the curiosity of the general public and the attention of the scientific community for its visual allure and structural complexity. A school is considered as a social aggregation of fish swimming in the same direction and maintaining nearly constant spacing with respect to neighbouring conspecifics [1]. This social swimming behaviour is common to a large spectrum of fish species [2]. It is recognized to produce an array of costs, such as increased sexual and feeding competition and parasitism [2], which can be outweighed by various advantages of group formation, including anti-predator behaviour, foraging, mate choice and reduced cost of transport [2–5]. These behaviours have been traditionally assumed to be generated in a self-organized manner in which all the school members behave like an egalitarian 'superorganism' [6–8]. However, a number of observations demonstrate large intrinsic variations among individuals in both behavioural and physiological traits [9–15]; this inter-individual variation may allow for the emergence of leadership in the gregarious group [16]. Although some experimental evidence has shed light on important aspects of schooling [2], the causes and consequences of leadership in schooling fish remain largely unexplored.

*Author for correspondence (mporfiri@poly.edu).

Electronic supplementary material is available at http://dx.doi.org/10.1098/rsif.2012.0084 or via http://rsif.royalsocietypublishing.org.

We hypothesize that the integration of a fish-like robot within a group of live fish may enable fundamental research on collective animal behaviour and open new directions at the interface of robotics and marine biology. In fact, the opportunity of controlling a member of a group may (i) provide valuable and multifaceted information on the feedback of live animals obtained by modulating the behaviour of this 'engineered' group member and (ii) enable novel conservation methods based on the controlled response of the group. Despite the potential of this approach, the relationship between bioinspired robots and live animals remains largely untapped [17–21]. Notably, biological studies on fish–robot interactions are limited to three-spined sticklebacks interacting with a fish-like replica rigidly dragged in a static environment [22–24]. However, none of these studies explore the interactions between animal systems and biomimetic robots whose locomotion mimics their animal counterpart in an authentic bioinspired design [25].

Here, we employ a robotic fish to study the interactions between animals and robotic devices. The robot biomimicry resides in its locomotion, as its propulsion system simulates the natural swimming performed by a fish and, as a consequence, is expected to create a wake pathway that can be exploited by live animals to reduce their energetic cost of movement [26]. We hypothesize that this high degree of biomimicry facilitates the acceptance of the robotic fish in a live fish school. In fact, one of the main advantages offered by swimming in a school is the hydrodynamic return that can be

Received 23 December 2011
Accepted 1 February 2012

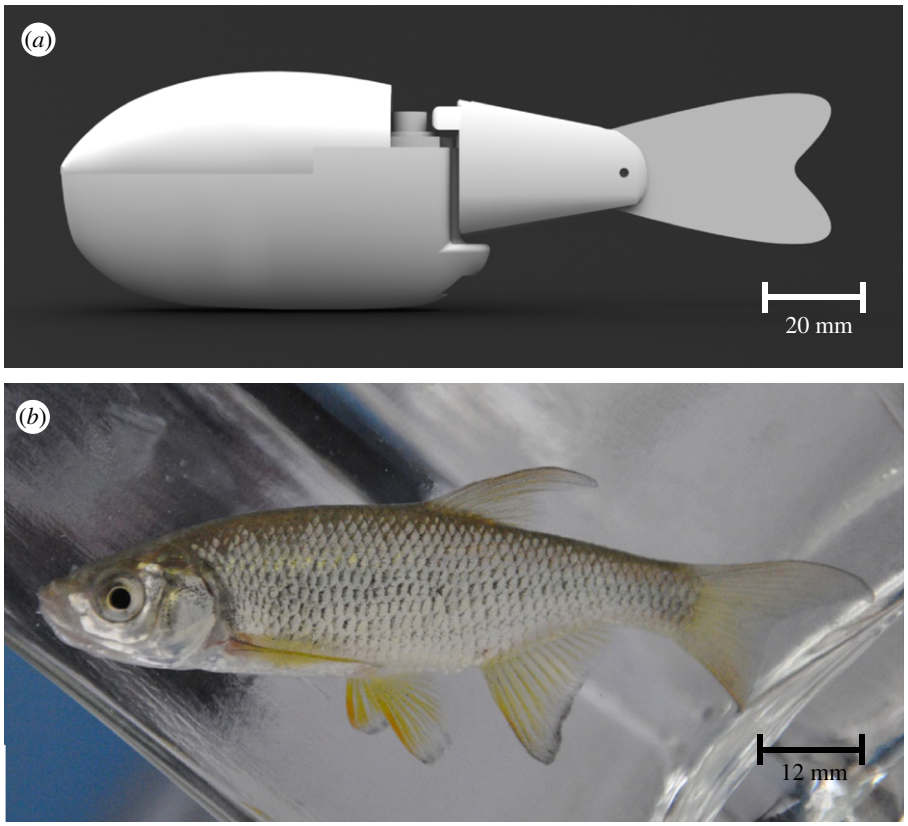

Figure 1. Illustration of the robotic fish and golden shiner with scale: (*a*) computer-aided design of the robotic fish and (*b*) picture of a golden shiner. (Online version in colour.)

obtained by individuals in the back positions as a consequence of the wake generated by individuals in front positions [4,15]. This benefit is evidenced by the tail beat frequency (TBF) reduction experienced by fish in the follower position that exploit the wake created by individuals in leading positions [15,27]; such frequency is directly related to energy expenditure during continuous swimming [4]. Therefore, a biomimetic robotic fish swimming in the school's front positions may provide a considerable hydrodynamic advantage to live fish in the trailing positions and thus effectively induce robotic leadership within the group.

In this study, we use a water tunnel to allow the robotic fish and individual golden shiners to swim together at different water velocities. Golden shiners are cyprinid fish native of North America of high ecological and economical relevance [28]. They are recognized to be highly gregarious fish, which makes this species an ideal experimental subject for this type of ethorobotics studies. We also use a digital particle image velocimetry (DPIV) system to characterize the flow physics. We test the hypothesis that, at certain swimming speeds, fish can be attracted by the biomimetic locomotion of the robotic fish and that this attraction depends on the hydrodynamic advantage induced by its swimming movement.

2. MATERIAL AND METHODS

2.1. Biomimetic robotic fish

The robotic fish used in this study is presented in the study of Abaid *et al.* [29] and its performance is studied by Kopman & Porfiri [30,31]. Briefly, it comprises a rigid acrylonitrile butadiene styrene (ABS) plastic body shell and a tail section constituted by a rigid ABS element and a compliant mylar caudal fin. The robot is designed in SolidWorks (figure 1*a*) and printed on a rapid prototyping machine (Stratasys, Dimension SST, USA). The robot is waterproofed with rubberized plastic. It has a length of 15 cm, a height of 4.8 cm and a width of 2.6 cm. The robot uses a waterproof servomotor (Traxxas, 2065 Sub-Micro servomotor, USA) to operate the tail section and achieve the desired biomimetic locomotion. The presence of a compliant caudal fin allows for a sinuous undulation of the tail mimicking live fish swimming. Robot tail beat frequency (TBF_{robot}) and tail beat amplitude (TBA_{robot}) are controlled by an external microcontroller (Arduino, Duemilanove, Italy). The signal driving the servomotor yields a periodic sinusoidal motion of the compliant mylar caudal fin.

2.2. Animals

Golden shiners, *Notemigonus crysoleucas* (length, 7.8 ± 0.5 cm; mass, 5.5 ± 0.3 g; mean $\pm$ s.d.) were obtained from a local fish farm (Bliss, NY, USA) in April 2011 (figure 1*b*). On arrival at the laboratory, fish were transferred to a holding tank with rectangular cross section (0.5 m^2) with re-circulating, filtered natural freshwater. Golden shiners were kept at constant temperature ($23 \pm 0.3^{\circ}$C) under prevailing natural photoperiod for at least three weeks before the beginning of the experiments. Fish were fed once a day

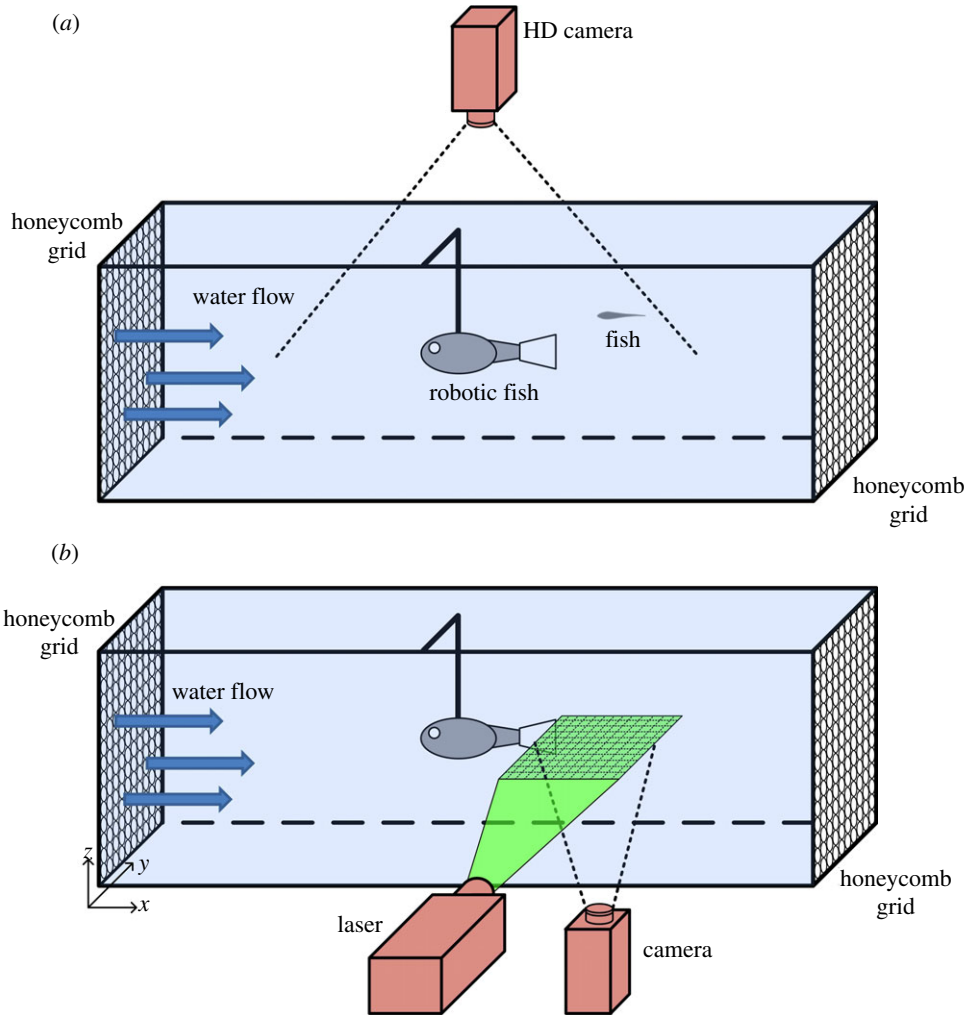

Figure 2. Schematics of the experimental setups. (*a*) Behavioural experiment: the robotic fish and individual golden shiners swimming in a section of a Blazka-type water tunnel delimited by two plastic honeycombs. A camera placed above the tunnel records their swimming. (*b*) DPIV analysis: the robotic fish swimming in a section of a Blazka-type water tunnel delimited by two plastic honeycombs. A laser sheet oriented in the horizontal (x,y) plane illuminates the seeded water in correspondence with the compliant mylar caudal fin. A camera placed below the tunnel records the area illuminated by the laser.

with goldfish granules (Aqueon, Franklin, WI, USA) and individuals were fasted for at least 24 h before use in experiments.

2.3. Experimental setup and protocol

Experiments are performed in a Blazka-type water tunnel (Engineering Laboratory Design, Inc., Lake City, MN, USA). The working section of the tunnel is 100 cm in length, 15 cm in width and 15 cm in height. Two plastic honeycomb grids delimit the working section and promote rectilinear flow and uniform velocity profiles. Water flow is generated by a variable speed electrical motor that allows for controlling the water velocity. The robot body shell is tethered to the middle of the experimental tank with a small metallic support rod; the centre of mass (CM) of the robot that is 6.5 cm from the tip of the nose is anchored at 50 cm from both the upstream and downstream ends of the section. A high-definition camera (Canon, Vixia HG20, Japan), filming at 30 frames per second, is placed above the working section to record the interaction between fish and the robotic fish (figure 2*a*). Fish are tested at 12 different conditions, identifying a combination of three water velocities (V1, 14; V2, 16; and V3, 28 cm s^{-1}) and four tail beat frequencies of the robotic fish (F0, 0; F1, 1; F2, 2; and F3, 3 Hz). A total of 72 fish were tested ($n = 6$ for each condition). We comment that even if V1 and V2 seem very close, they actually differ by one-quarter fish body length (BL) per second, which is expected to produce significant differences in TBF of fish of this size [32].

The experiment starts with an individual fish transferred from the holding tank to the water tunnel. The water velocity at the time of the transfer is zero while the tail of the robotic fish is already beating at the desired frequency. After 2 min, the water velocity is increased from zero to approximately half of the final water velocity (for example, 7 cm s^{-1} in the case of a final velocity of 14 cm s^{-1}). After 30 min, the water velocity is increased to the final testing value. Fish are left undisturbed for another 30 min and then their swimming with the robotic fish is recorded for 5 min. At the end of these 5 min, fish are removed from the water tunnel and measured for length and weight before being placed in a different holding tank.

In separate experiments, DPIV is used to characterize the hydrodynamics of the wake generated by the robotic fish at the 12 different swimming conditions obtained by varying the water velocity and TBF_{robot} (figure 2*b*). The implementation of this method follows standard fluid dynamics practice, as shown, for example, in the study of Peterson *et al.* [33]. Briefly, the water is seeded with silver-coated hollow glass microspheres (17 μm diameter, Potters Industries, Inc., Carlstadt, NJ, USA), which are illuminated by a double-pulsed NewWave Solo III 100 mJ per pulse Nd:YAG laser. A horizontal laser sheet of approximately 1 mm thickness is spread along the central axis of the tail of the robotic fish. A 1000×1000 pixel^2 RL Megaplus ES 1.0 camera with an AF Micro Nikkor 60 mm focal length lens is used to capture images. The field of view is 200×150 mm^2. A Dantec Dynamics FlowMap 1500 system (Dantec Dynamics A/S, Tonsbakken, Denmark) synchronizes the camera and the laser and processes the images. Sequential pairs of video images (4 ms apart in time) are collected and analysed using cross correlation to estimate the two-dimensional water velocity field in the plane of observation [34]. The bulk displacement of particles in a small interrogation region between the two images is used to approximate the velocity in that region at the time instant of the first image. Image pairs are cross-correlated using the FlowManager processing software (Dantec Dynamics A/S, Tonsbakken, Denmark). The cross-correlation analysis uses a multi-pass central difference fast-Fourier transform correlation process with a final interrogation region size of 16×16 pixels^2 with 50 per cent overlap [35].

Figure 3 illustrates the field of view in DPIV experiments along with the region of interest whose velocity field is plotted in the following analysis. In addition, figure 3 displays the CM of the robot with two lines emanating from this point to show the neutral position of the tail and a feasible angular position of a following fish. For each of the 12 conditions, 75 pairs of images are collected. Three complete tail beats of the robotic fish are considered in the analysis, resulting in different numbers of image pairs analysed at the different TBF_{robot}, that is, 45 at 1, 28 at 2 and 16 at 3 Hz. Thirty image pairs are analysed at the TBF_{robot} of 0 Hz.

Note that, in the present experiment, the behavioural (fish–robot interaction) and hydrodynamic (DPIV measurements) analyses were not conducted together. This was mainly done to avoid potential bias owing to the presence of a pulsating and high-intensity laser sheet that can affect fish behaviour. We expect that the larger size of the robot and the three-dimensional structure of the wake from its tail [36] would not alter significantly the main features of the flow physics reported in this study if live fish were swimming with the robot at a relatively large distance [37].

2.4. Behavioural and hydrodynamic measurements

Swimming sequences are analysed using Redlake MotionScope PCI (v. 2.21.1.). For each 5 min-long video, 60 snapshots are taken at 5 s intervals. Two-dimensional x and y Cartesian coordinates of the robot's and fish's centres of mass are acquired for each snapshot with the x-axis along the length of the working section of the tunnel for convenience. A live fish is considered to interact with the robot whenever the x-coordinate of its CM is in a region (R) that extends to 4 BL from the x-coordinate of the CM of the robot (CM_{robot}). R occupies approximately 60 per cent of the total area available for fish to swim in the water tunnel. The CM of each fish is estimated to be at 38 per cent of its total length from the tip of the head. In addition, we partition the domain R into the front (R^{ft}) and the back (R^{bk}) regions (figure 4). Specifically, R^{bk} identifies the portion of the observation region in which the robotic fish mostly perturbs the flow; the perturbation is induced by the tail beating, which, in turn, creates vortical structures. This region is assumed to begin at 4 cm from CM_{robot} along the x-axis, corresponding to the end of the rigid element of its tail section. R^{ft} is considered as R deprived of R^{bk}.

To describe the level of attraction of an individual fish towards the robot, we measure the time spent by a fish within R (τ) and the time spent within R^{bk} (τ^{bk}). For each condition, we average these individual-based variables to learn about the overall ability of the robot to attract fish. Specifically, we define the mean time spent by the fish within R ($\bar{\tau}$) and the mean time spent by the fish within R^{bk} ($\bar{\tau}^{bk}$) ($n = 6$). To investigate the correlation between fish attraction to the robot and swimming patterns, we measure the individual fish TBF, when swimming both in R^{ft} (TBF^{ft}) and R^{bk} (TBF^{bk}). When possible, four blocks of 5 s are analysed for each condition and for each fish to estimate these variables. We subtract TBF^{ft} or TBF^{bk} from TBF_{robot} to quantify the mismatch between the robot and the fish TBF when swimming in R^{ft} (Δf^{ft}_{robot}) or in R^{bk} (Δf^{bk}_{robot}).

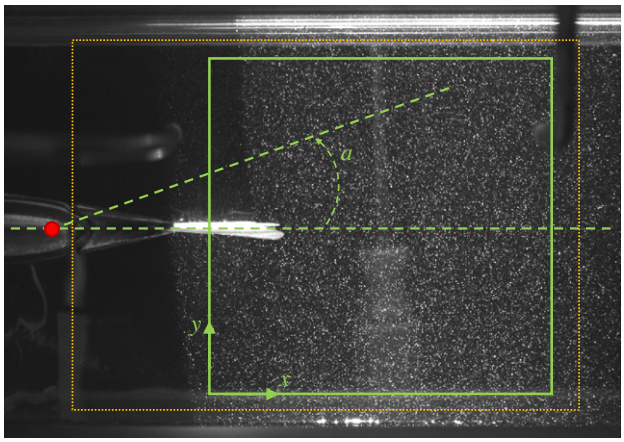

Figure 3. Picture from DPIV analysis illustrating the tail of the robotic fish and seed particles illuminated by the laser sheet. Superimposed dotted orange lines identify the region where DPIV analysis is performed and superimposed solid green lines define the region for which flow data are presented using displayed x- and y-coordinates. Superimposed red dot represents the centre of mass of the robot and dashed green lines define the tail rest position and a representative direction at the back of the robot for which the angle a is defined. (Online version in colour.)

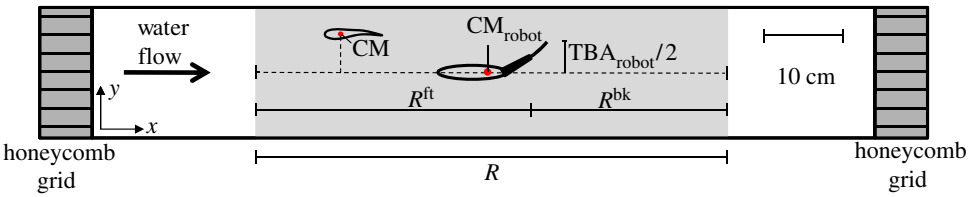

Figure 4. Top view of the water tunnel with schematic illustration of some of the experimental variables. CM_{robot} represents the centre of mass of the robotic fish. CM represents the centre of mass of the fish. A live fish is considered to interact with the robot whenever the x-coordinate of its CM is in a region (R; section in grey), which extends 4 BL from the x-coordinate of CM_{robot}. R is additionally partitioned into the front (R^{ft}) and the back (R^{bk}) regions. (Online version in colour.)

For each water velocity, we take the mean of TBF^{ft} and TBF^{bk} over the whole set of fish tested at that water velocity ($n = 24$) to obtain the average TBF when either leading or following the robot. For overall comparison, we also consider the average TBF for a selected water velocity as the mean of these two averages. In addition, for each fish, we define Δf as the difference between its specific TBF^{bk} and the average TBF^{ft} corresponding to that water velocity.

To further characterize the attraction of fish to the robot, for each behavioural trial, we compute the polar coordinates of the fish with respect to the robot by setting the origin at the robot's CM and taking null angle if the fish is aligned with the robot. From these angular coordinates, we measure the so-called mean circular vector which ranges from 0, corresponding to the fish attaining all feasible angles throughout the trial, to 1, when its angle is held constant [38]. Note that, in this computation, angles are normalized between 0° and 180° to account for the symmetry. We say that the fish holds station with respect to the robot when its mean circular vector is higher than 0.95 and we report the mean angle (a) for completeness (figure 3). If such mean angle is less than 90°, we say that the fish holds station behind the robot. We comment that this quantity is computed within R, that is, a fish may hold station with respect to the robot even if it does not stay in R for the whole duration of the experiment. Yet, this quantity is only computed for fish that spend at least 70 per cent of the 5 min observation period within R.

Finally, to characterize the robot propulsion, we measure its tail beat amplitude (TBA_{robot}). This quantity is used to compute the oscillatory Reynolds number of the beating tail that is directly related to the thrust produced by the biomimetic propulsor [39]. Specifically, the oscillatory Reynolds number is $Re = TBA_{robot}\, TBF_{robot}\, 2\pi l/\nu$, where l is the length of the whole actuator comprising both the rigid and the compliant tail and ν the water kinematic viscosity. In SI units, the average thrust per unit width is computed as $T = 7.81 \times 10^{-10}\, Re^{2.07}$; therefore, the speed of the robot if it were swimming in quiescent water can be estimated by [40]:

$$V = \sqrt{\frac{2Tw}{C_D \rho L^2}},$$

where w is the fin width, L the robot length, ρ the water mass density and C_D is the drag coefficient which is estimated to be 0.275 from the identification of free swimming data [31]. Note that this estimate uses the so-called statically balanced thrust [41] and neglects the yaw motion of the vehicle body [40] to compute the robot's terminal speed. Alternative estimates for the terminal speed based on slender body theory can be found in the study of Chen *et al.* [42].

For convenience, we normalize V with respect to the water velocities. Values proximal to 100 per cent indicate that the robotic fish would be able to remain in constant position at the given water velocity without the support of the rod. Values above and below 100 per cent represent cases where the robotic fish would move upstream or downstream, respectively, compared with its original position in the tunnel.

The velocity intensity field and the vorticity are calculated using a custom-designed code in Mathematica 8 (Wolfram, Champaign, IL, USA).

2.5. Statistical analyses

A two-way ANOVA, having water velocity and TBF_{robot} as independent factors and the time spent within 4 BL from the robot (in seconds) as dependent variable, is used to evaluate whether fish preference to stay within R varies significantly between the test conditions [43]. A two-way ANOVA, with TBF as the dependent variable and independent variables given by the water velocity and the x-position relative to the robotic fish, is performed to determine whether TBF differs as the water velocity changes and whether it is computed in R^{ft} and R^{bk}. Linear regressions are performed to investigate the relationships between τ and τ^{bk} and Δf, Δf^{ft}_{robot} and Δf^{bk}_{robot}. Statistical analyses were performed using SigmaPlot v. 11.0, and Mathematica 8. A probability less than 5 per cent ($p < 0.05$) is taken as the limit for statistical significance.

3. RESULTS

Interactions between fish and robot are observed to depend strongly on the experimental conditions (figure 5; $n = 6$). In particular, at $TBF_{robot} = 0$ Hz, fish spend relatively less time within 4 BL of distance from the robotic fish, that is, in R (ranging from 5.5 to 15.3% with a mean of 10.1%), than at TBF_{robot} of 1, 2 and 3 Hz (ANOVA, $p < 0.05$; post-hoc tests: $TBF_{robot} = 0$ Hz versus $TBF_{robot} = 1$ Hz, $p < 0.05$; $TBF_{robot} = 0$ Hz versus $TBF_{robot} = 2$ Hz, $p < 0.05$; $TBF_{robot} = 0$ Hz versus $TBF_{robot} = 3$ Hz, $p < 0.01$). Fish tend to spend more time closer to the robotic fish at certain combinations of TBF_{robot} and water velocities,

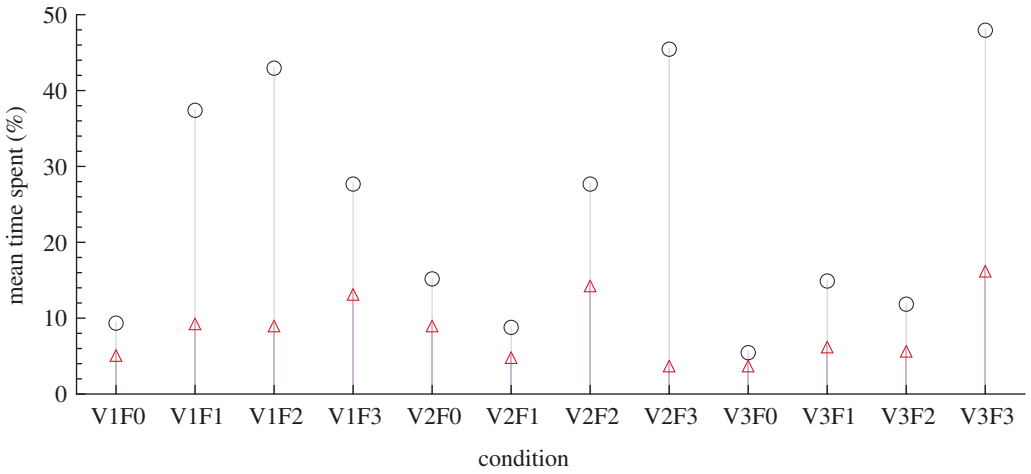

Figure 5. Mean time spent within 4 BL to the robotic fish at the 12 different conditions ($n = 6$ at each condition) scaled with respect to the total acquisition time. Black empty circles represent the mean time spent when swimming in R ($\bar{\tau}$) at each of the 12 conditions. Red empty triangles represent the mean time spent in R^{ft} ($\bar{\tau}^{\mathrm{ft}}$) for each of the 12 conditions. (Online version in colour.)

in particular at V1F1, V1F2, V2F3 and V3F3 (37.5, 43, 45 and 48.3%, respectively; $n = 6$ at each condition).

When fish swim in R, there is no statistical preference to swim in its front or back position (ANOVA, $p > 0.05$) except in these four preferred conditions (that is, V1F1, V1F2, V2F3 and V3F3; ANOVA, $p < 0.05$; figure 5). Among these conditions, seven fish hold station behind the robot (V1F1: one fish with $\tau = 91.6\%$, $\tau^{\mathrm{bk}} = 80\%$, $\mathrm{TBF}^{\mathrm{bk}} = 3.05$ Hz, $a = 44.2^{\circ}$; V1F2: one fish with $\tau = 71.7\%$, $\tau^{\mathrm{bk}} = 70\%$, $\mathrm{TBF}^{\mathrm{bk}} = 3.21$ Hz, $\mathrm{TBF}^{\mathrm{ft}} = 3.52$ Hz, $a = 33.5^{\circ}$ and a second fish with $\tau = \tau^{\mathrm{bk}} = 100\%$, $\mathrm{TBF}^{\mathrm{bk}} = 2.5$ Hz, $a = 38.3^{\circ}$; V2F3: two fish with both $\tau = \tau^{\mathrm{bk}} = 100\%$, $\mathrm{TBF}^{\mathrm{bk}} = 3.96$ and 3.7 Hz, $a = 31.5^{\circ}$ and 33.8°, respectively; and V3F3: one fish with $\tau = 98.7\%$, $\tau^{\mathrm{bk}} = 83.3\%$, $\mathrm{TBF}^{\mathrm{bk}} = 3.9$ Hz, $\mathrm{TBF}^{\mathrm{ft}} = 4.3$ Hz, $a = 39.1^{\circ}$ and a second fish with $\tau = 78.3\%$, $\tau^{\mathrm{bk}} = 65\%$, $\mathrm{TBF}^{\mathrm{bk}} = 4.2$ Hz, $a = 50.9^{\circ}$). In other words, they persistently occupy the same microhabitat for a substantial portion of the observation period as displayed in figure 6. In the remaining conditions, fish swim at the back of the robot without maintaining a fixed angle as further illustrated in figure 6.

We also find that TBF increases significantly as the water velocity increases (average TBF at V1, 3.3 Hz; average TBF at V2, 4.1 Hz; average TBF at V3, 4.5 Hz; ANOVA, all $p < 0.05$). At V1, there is a significant difference between TBF measured when swimming in R^{ft} and R^{bk} (R^{ft} higher than R^{bk}; ANOVA, $p < 0.05$; figure 7), which is not found at V2 and V3 (ANOVA, both $p > 0.05$; figure 7).

Figure 8 shows a positive significant relationship between Δf and the time spent swimming in R^{bk} (linear regression, $p < 0.05$; $n = 29$). Individuals with a higher reduction in their TBF when swimming in R^{bk}, compared with the average values for swimming in R^{ft}, spend more time in the robot's back. Notably, the seven individuals that are found to hold station behind the robot are all characterized by a reduction in TBF as quantified by a positive value of Δf. Figure 9 shows a positive significant relationship between both $\Delta f^{\mathrm{ft}}_{\mathrm{robot}}$ and $\Delta f^{\mathrm{bk}}_{\mathrm{robot}}$ and τ^{bk} (linear regression, front position $p < 0.05$; back position $p < 0.01$). This graph shows how individuals whose TBF is closer to that of the robotic fish are more prone to spend time in its proximity, however TBF is never synchronized with $\mathrm{TBF}_{\mathrm{robot}}$ (figure 10).

The robotic fish is able to sustain its swimming at four of the different conditions tested in this experiment, that is, its normalized velocity is close to 100 per cent at V1F2, V1F3, V2F2 and V2F3 (figure 11). Notably, two out of four of these conditions (that is, V1F2 and V2F3) are those where fish hold the station at the back of the robotic fish.

Figure 12 displays representative results of DPIV in the vicinity of the robot tail for all test conditions. Specifically, it shows the average intensity of the velocity field ($|\bar{V}_{\mathrm{ave}}|$) computed by averaging over the entire sequence of frames for the considered conditions. The beating of the tail induces a very different average intensity field characterized by the formation of two water jets symmetrically oriented with respect to the neutral position of the tail vibration, similar to those observed for electro-active polymers vibrating in quiescent fluids as shown in the study of Peterson *et al.* [33]. The time-resolved analysis of the vorticity field generated by the tail beating of the robot is presented in figure 13 for conditions V1F1, V1F2, V2F3 and V3F3, where some fish are found to hold station at the back of the robot.

4. DISCUSSION

Our results reveal that the biomimetic locomotion of the robotic fish is a determinant of fish positional preference. In fact, live fish tend to spend more time close to the robotic fish when its tail is beating rather than when it is statically immersed in the water as a 'dummy'. At some particular combinations of water velocity and $\mathrm{TBF}_{\mathrm{robot}}$, some fish hold station behind the robot. That is, they specifically occupy a narrow range of angular positions aligned with water jets that are

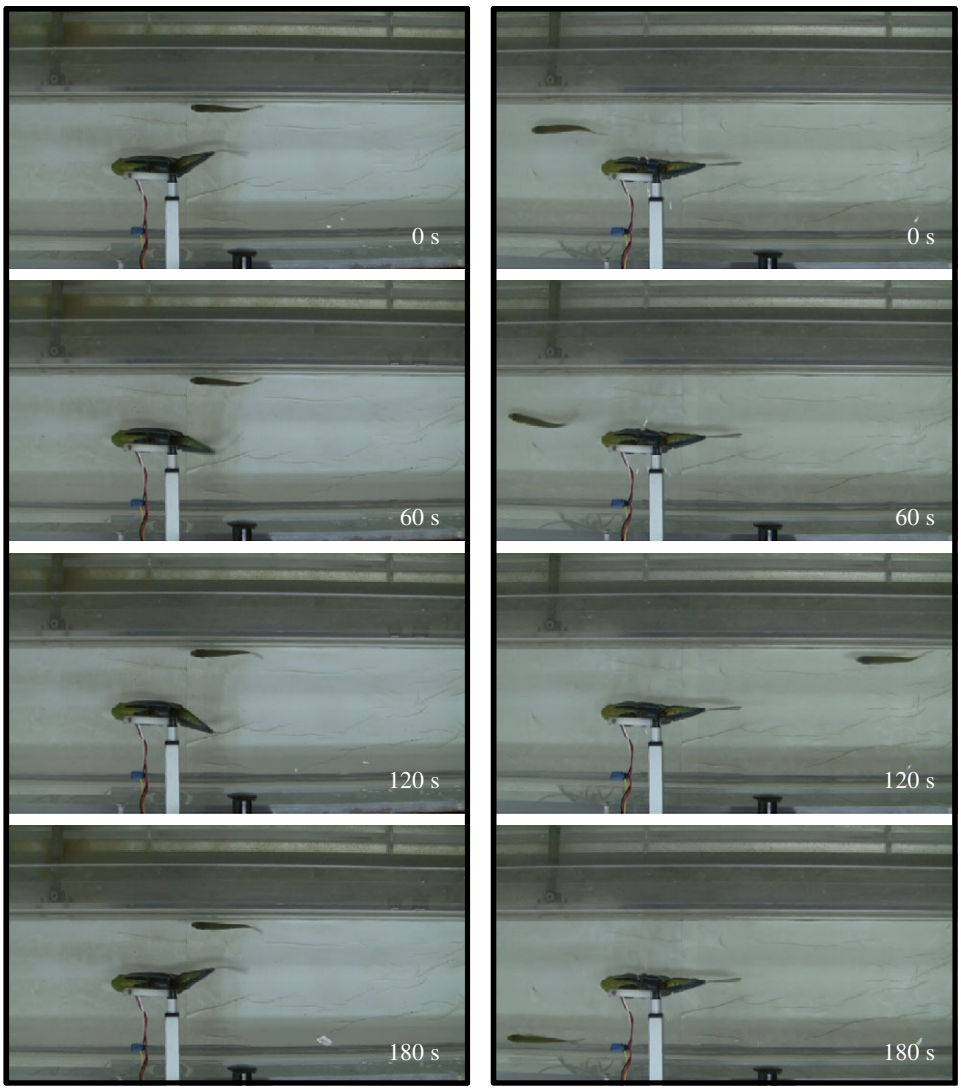

Figure 6. Examples of fish swimming with robotic fish at different conditions. The left column shows four snapshots from V1F2 at different time of the experiment. Fish swimming at this condition tend to hold station behind the robot. (See electronic supplementary material.) The right column shows four snapshots from V1F0 at different time of the experiment. Fish swimming at this condition swim randomly around the robotic fish. (Online version in colour.)

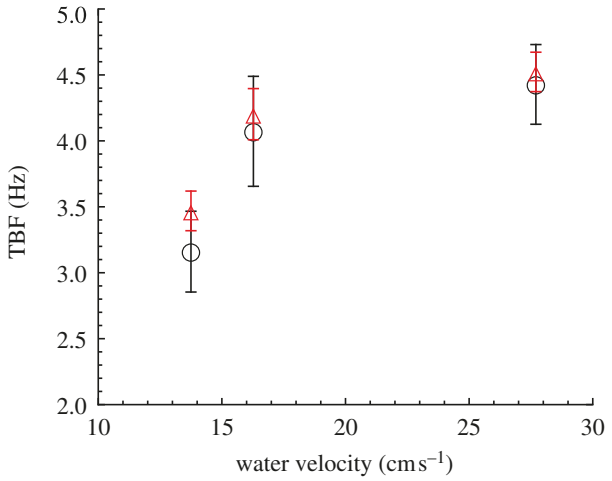

Figure 7. TBF measured at different speeds. TBF increases as water velocity increases. Black empty circles represent TBF measured when swimming in R^{bk} at 14, 16 and 28 cm s^{-1}. Red empty triangles represent TBF measured when swimming in R^{ft} at these three different water velocities. (Online version in colour.)

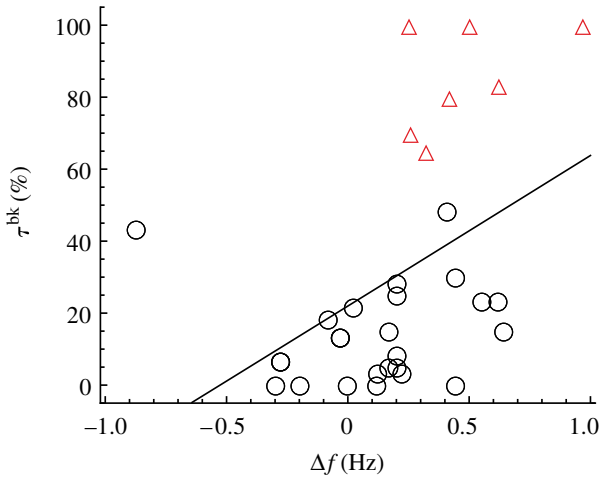

Figure 8. Relationship between Δf and τ^{bk} scaled with respect to the total acquisition time (linear regression: $y = 21.9 + 41.8x$, $r^2 = 0.2$, $p < 0.05$, $n = 29$). Red empty triangles identify individuals that hold station behind the robot. (Online version in colour.)

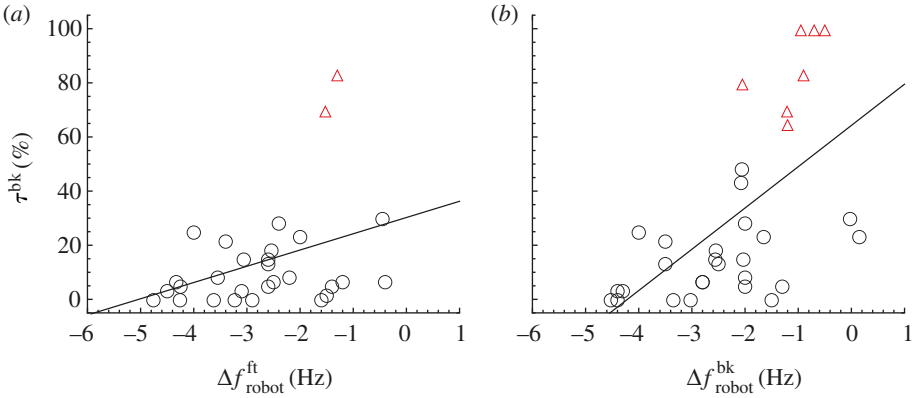

Figure 9. Relationship between Δf_{robot} measured in both (*a*) front and (*b*) back position and τ^{bk} scaled with respect to the total acquisition time (linear regression, front position, $y = 30.2 + 6x$, $r^2 = 0.13$, $p < 0.05$, $n = 29$; back position, $y = 64.2 + 15.3x$, $r^2 = 0.36$, $p < 0.01$, $n = 32$). Red empty triangles identify individuals that hold station behind the robot. (Online version in colour.)

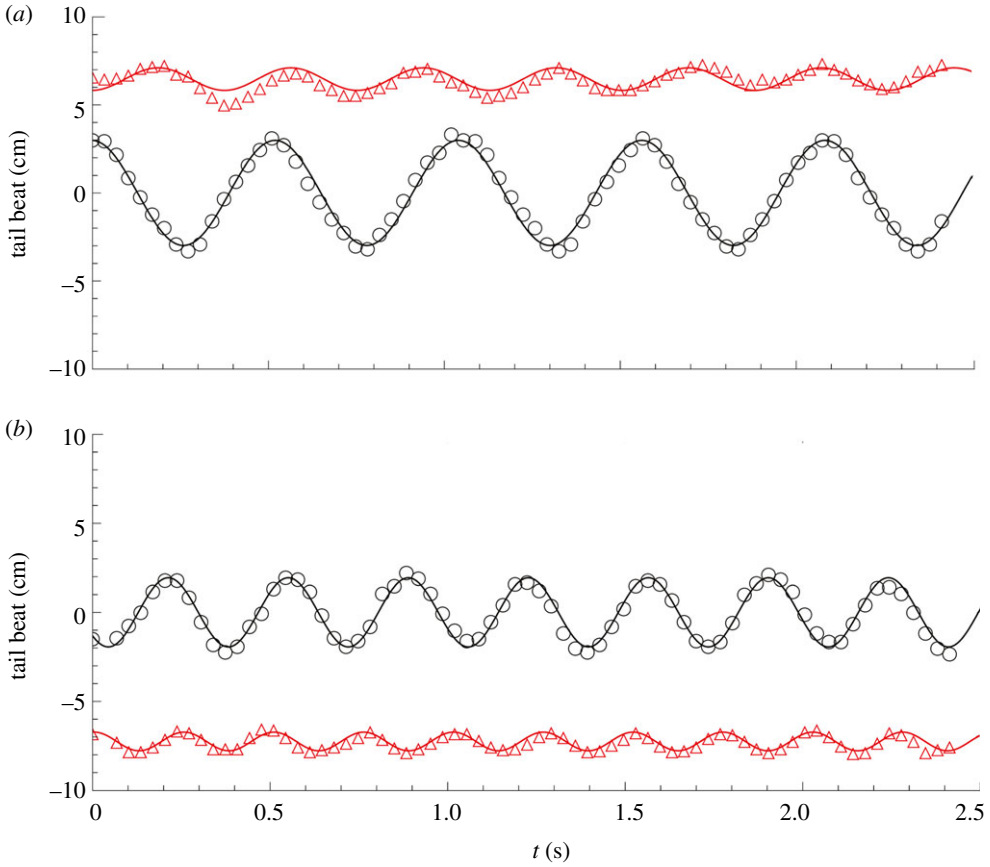

Figure 10. Examples of traces of the tail movement of the robotic fish (black empty circles) and the fish (red empty triangles) when swimming together in the water tunnel at (*a*) 14 cm s^{-1} with $TBF_{robot} = 2$ Hz (V1F2) and at (*b*) 16 cm s^{-1} with $TBF_{robot} = 3$ Hz (V2F3). Solid lines represent sinusoidal fits of the tails' movements. (Online version in colour.)

generated by the flapping tail. This restricted microhabitat appears to be the place where individuals can obtain a hydrodynamic advantage that potentially reduces energy expenditure during their swimming. This suggests that, in non-static flows, interactions between this class of robotic fish and golden shiners are dominated by hydrodynamic cues more than visual attraction.

When one or more members of a fish school are dominant over others as a result of some behavioural, physiological and/or ecological pressure, leadership and followership are likely to appear [11,16,44,45]. For example, during migration, individuals having higher aerobic capacity (that is, total capacity for oxygen supply to tissues and ATP production, for use in all oxygen-consuming physiological functions within an organism at a given time) tend to occupy front positions and, *vice versa*, individuals with lower aerobic capacity are more prone to occupy back positions [15]. This phenomenon occurs because individuals in trailing positions can reduce their TBF [15] and, as a consequence,

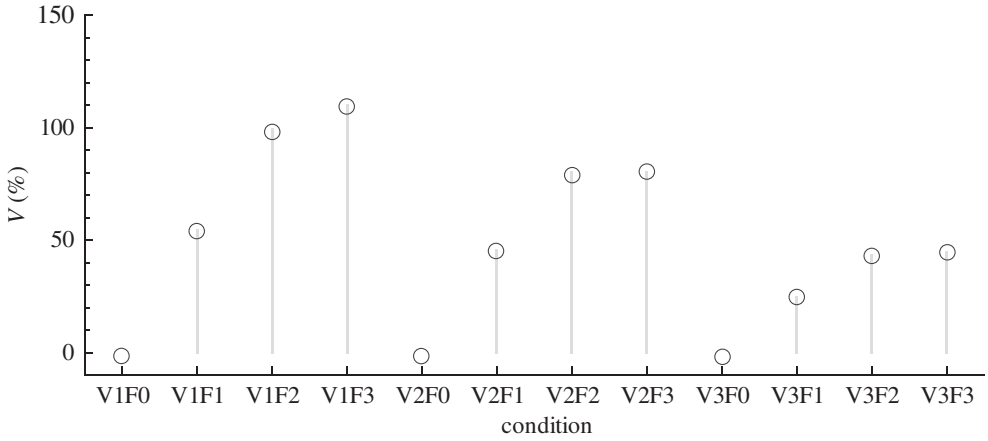

Figure 11. Velocity of the robot at the different conditions normalized with respect to the water velocity.

their energy expenditure [4]. In our experiment, we analogously find that individuals taking follower positions with respect to the robot are those that maximize Δf and hence are expected to obtain the highest energy saving (figure 8). However, when the data on the reduction in TBF are averaged across the whole fish population differences are difficult to track. This is evidenced in figure 7, where the statistical differences are displayed only for V1, which accounts for two out of the four preferred conditions.

Fish tendency to swim at the back of the robotic fish may be caused by the flow physics induced by the robot's biomimetic locomotion, which is exemplified through figure 12, where the existence of flow jets emanated by the robotic tail is demonstrated. The time-resolved analysis of the flow physics downstream of the robot illustrated in figure 13 shows that these jets correspond to a train of vortical structures generated in the proximity of the beating tail and shed downstream by the imposed channel flow. Notably, the intensity and frequency of these vortical structures are similar to the linked vortex rings generated by the caudal fin of real fish during their swimming [46,47]. Previous works have shown that fish can exploit vorticity patterns, such as the Karman vortex street, that are generated by unsteady flow separations resulting in the formation of vortex pairs travelling downstream [26], to reduce their oxygen uptake and consequently their energy expenditure during swimming [48]. Our experiment seems to confirm these findings, as we observe that fish tend to hold position at regions close to the robotic fish tail characterized by high vorticity following a spatial formation that is similar to the diamond structure employed by conspecifics when swimming in school [49]. Specifically, we find that all the individuals holding station behind the robot reside in the same region characterized by the range of between 30° and 50° (see figure 3 for comparison; note that values are from 0° and 180°, so that fish angular position is independent of whether fish stay on the left or the right of the robot). By superimposing such positions and the vorticity field induced by the robot's tail beating as shown in figure 13, we find that the individuals that held station behind the robot always occupied regions where the vorticity changes mostly in time. Therefore, it is reasonable to assume that the robotic fish's biomimetic movement is generating vorticity patterns which are exploited by the live animals to reduce their energy expenditure. While prominent vorticity patterns are generated in all the conditions where the robot is beating its tail, the attraction of fish towards the robot is stronger when their TBF is closer to $\mathrm{TBF}_{\mathrm{robot}}$, that is, when the shedding of vortical structures from the robot tail matches the natural frequency of live fish. This finding is in line with the observation of frequency synchronization of rainbow trout with the shedding frequency of Karman vortex streets [48].

However, we note that not all of the individuals in this study interact with the robotic fish in the same way. Some of the fish did not hold station downstream of the robotic fish, even when swimming at those particular conditions that are favourable to others. A possible explanation why individuals differ in their degree of interaction with the robotic fish is that differences in their metabolic physiology may drive individuals with higher aerobic capacity to swim in front of the robotic fish. Having higher aerobic capacity demands higher food intake rates [50,51] and the frontal position in a school can give this foraging advantage. Moreover, a major benefit of higher aerobic capacity is given by the ability of swimming at higher speeds while keeping enough energy to feed and digest. Another possible explanation may reside on fish perception of the robot. Specifically, the robot can be perceived as a predator by some fish and individuals may react differently to such threat. Thus, different levels of threat perception may influence fish positioning with respect to the robot. This hypothesis may find additional support from the fact that golden shiners are extensively used as bait fish for recreational fishing and that the robot is approximately twice the size of fish (figure 1). For some fish, the disparity in size may promote the attraction towards the robot rather than avoidance, if the robot were perceived as a conspecific of larger body size [52]. We comment that such difference in size is difficult to reduce given the number of hardware components needed to allow the untethered operation of this robot [30].

Although some previous works have successfully investigated the interactions between live animals and

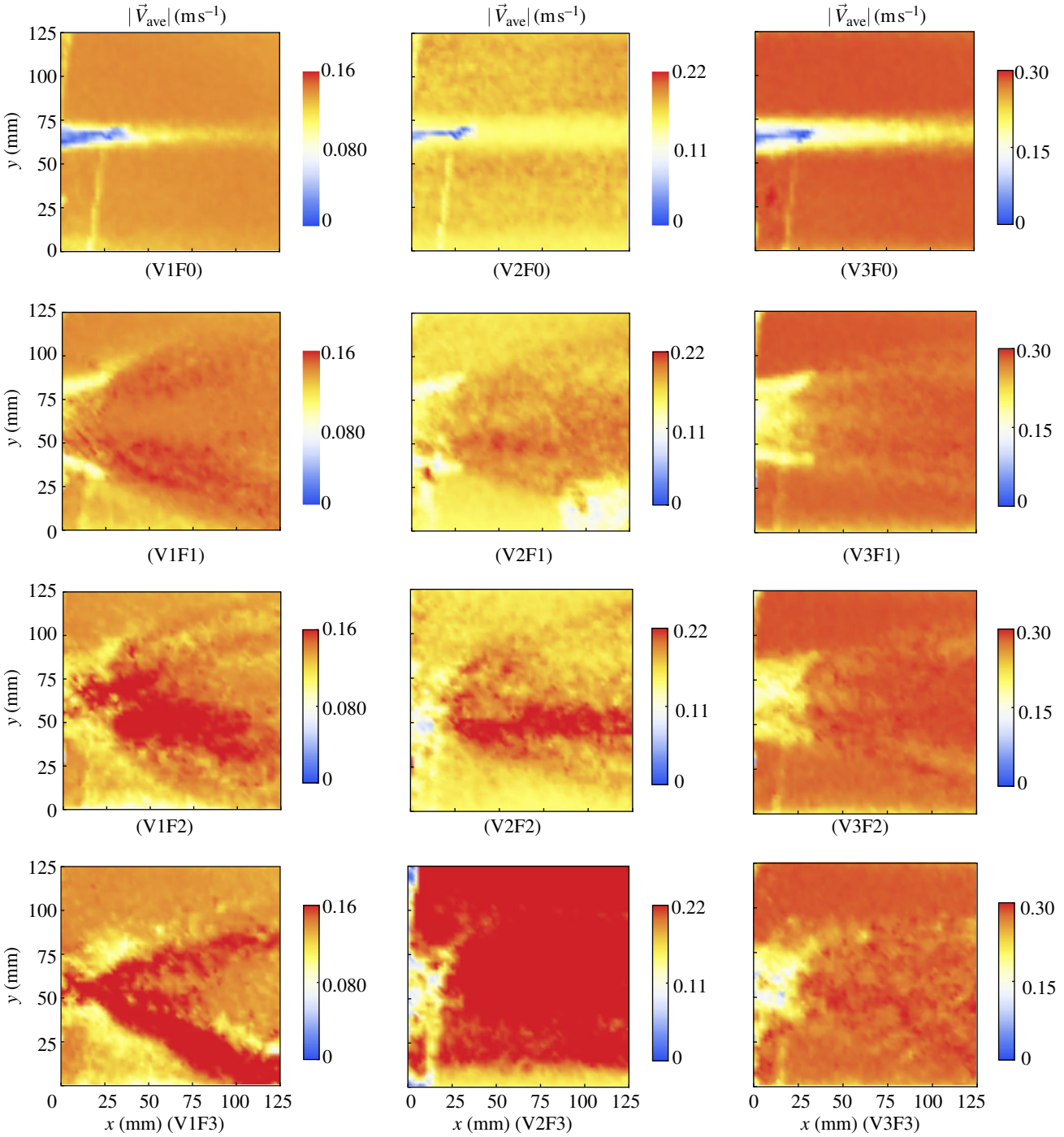

Figure 12. Velocity intensity in the vicinity of the flapping robot tail averaged over the entire sequence of frames for all conditions. Note that the first row represents the case of $\mathrm{TBF}_{\mathrm{robot}} = 0$ Hz. The region of observation corresponds to the area identified in figure 3.

robots or animal-like replicas, none of these studies have considered robots that are designed to simulate animal locomotion. For example, Vaughan *et al.* [18] have developed a sheepdog-like robotic device that is able to drive ducks to a predefined region in the area of experimentation. Halloy *et al.* [20] have used pheromones to allow the acceptance of autonomous robots in a group of cockroaches. Partan *et al.* [21] have analysed the interactions of eastern grey squirrels with replicas displaying alarm behaviour. Takanishi *et al.* [17] have studied interactions of a miniature ground vehicle with rats. Faria *et al.* [22] have used a fish-like replica, controlled with a magnet placed under the tank, to visually attract and drive single fish out of a refuge and to initiate new swimming directions in both individuals and groups. The novelty of our work resides in the use of a robotic fish that is able to mimic fish swimming and thus create hydrodynamic advantages analogous to conspecifics. The fact that live fish are attracted to the robot only when it beats its tail suggests that, in non-static flows, hydrodynamic advantages induced by the robotic fish's biomimetic locomotion may overcome other cues, such as visual attraction [53]. In other words, while the robotic fish

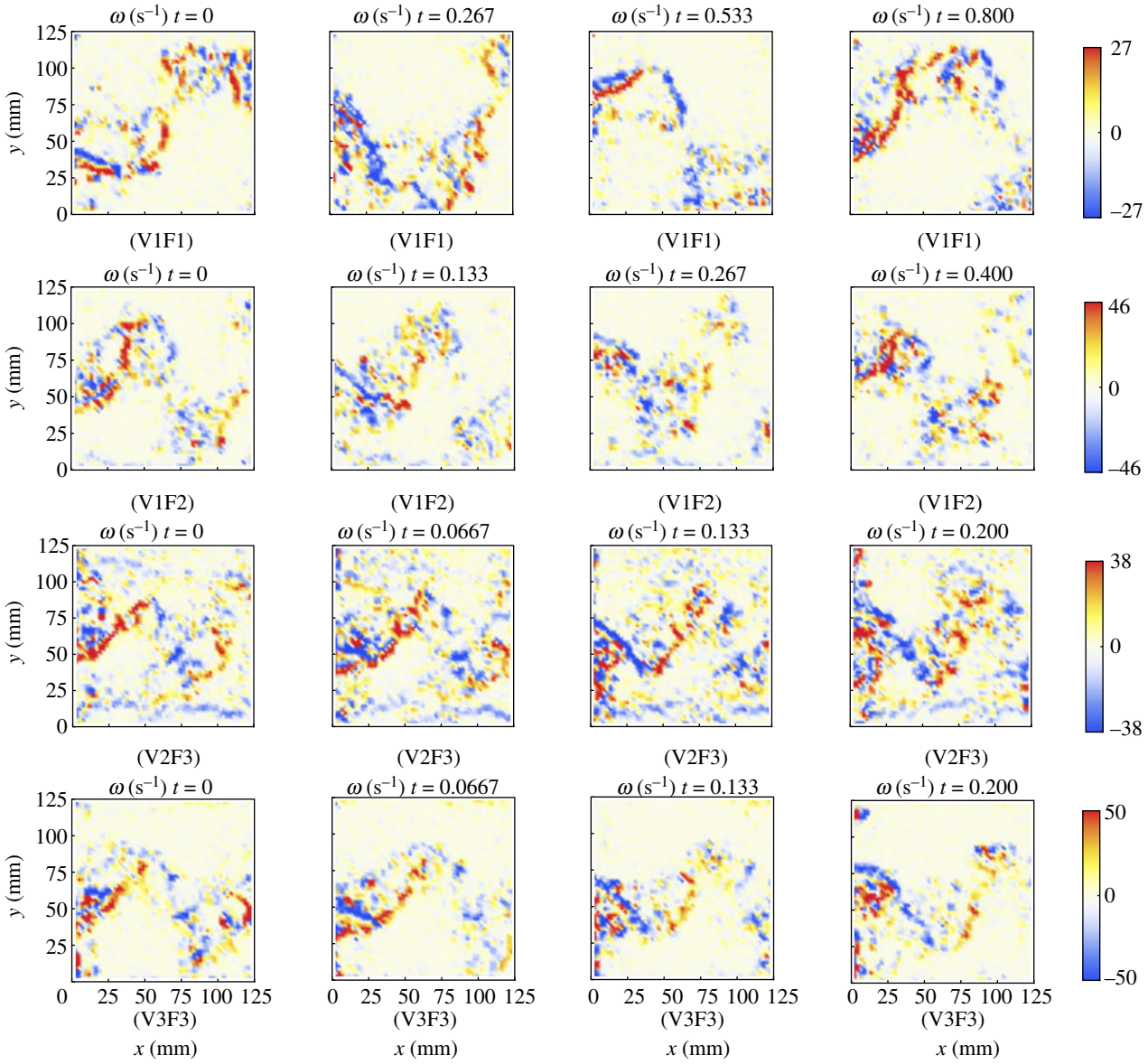

Figure 13. Time-resolved vorticity field induced by the robot's tail beating for the conditions where some of the fish hold station at its back. Red structures represent counterclockwise vortices; blue structures represent clockwise vortices. The region of observation corresponds to the area identified in figure 3.

attracts only a portion of the live fish when beating its tail (the average time spent in R is at most 48.1%), such attraction is almost completely lost when it is immobile.

In this experiment, we have tested animal–robot interaction for 1 h acclimation and 5 min recording; however, as fish may reduce their swimming cost by exploiting the robotic fish swimming, we can speculate on the possibility that fish can be led by the robotic fish for prolonged periods of time. Further work should investigate the temporal stability of our findings over extended time windows suitable for experimentation in the wild. We also comment that, in our experiment, the robotic fish was attached to the water tunnel with a metallic rod to allow for a systematic spatial characterization of the fish–robot interaction in a broad range of $\mathrm{TBF}_{\mathrm{robot}}$ and water velocities and to favour a standard field of view for the camera during the DPIV measurements. Nonetheless, the robot is able to swim freely as documented earlier [30] and, if left free to swim, it would be able to sustain its swimming at four of the different conditions tested in this experiment (that is, V1F2, V1F3, V2F2 and V2F3) including two conditions for which fish hold station with respect to the robot. We further note that the selected experimental design tends to emphasize hydrodynamic phenomena versus behavioural choices owing to the presence of a mean flow in which fish are forced to swim and thus interact with the vortical structures generated by the swimming robot, which is held stationary in the water tunnel. Further information about the leadership of such robot should be garnered by using alternative experimental designs focused on behaviour, such as the methodology used in the study of Reebs [52] to study the influence of body size on leadership.

Nature is a growing source of inspiration for engineers. This study has demonstrated that the degree of biomimicry in the robotic locomotion has a major role

in determining the feasibility of attracting live fish in non-static flows. Introducing biomimetic robotic devices in the wild may open new horizons for conservation studies. If accepted by the animals, robotic fish may act as leaders and drive them away from human-induced ecological disasters that are affecting life in aquatic environments, such as oil spills, and man-made structures, such as dams. In addition, such robots can be used in the laboratory to design experiments addressing fundamental questions in animal behaviour. With reference to collective behaviour, the use of 'engineered' group members controlled by the researcher may allow to test a wide spectrum of hypotheses pertaining to hierarchies in spatial positioning with respect to energetic, morphological, and behavioural traits of individual fish.

This material is based upon work supported by the National Science Foundation under (grant no. CMMI-0745753). The authors thank Vladislav Kopman for technical support on the robotic fish and the figures, James Tsao for help with schematics' preparation, Matteo Aureli for providing help with the DPIV analysis and figure preparation, and Nicole Abaid and Dr Sean D. Peterson for useful comments on the manuscript. The authors would also like to express their gratitude to two anonymous reviewers and Dr Stephan G. Reebs for their careful reading of the manuscript and for giving useful suggestions that have helped improve the work and its presentation. The experiment described in this work was approved by Polytechnic Institute of New York University Animal Welfare Oversight Committee AWOC-2011-101.

REFERENCES

1 Pitcher, T. J. & Parrish, J. K. 1993 Function of shoaling behaviour in teleosts. In *Behaviour of teleost fishes* (ed. T. J. Pitcher), pp. 363–439. London, UK: Chapman & Hall.
2 Krause, J. & Ruxton, G. D. 2002 *Living in groups*. Oxford, UK: Oxford University Press.
3 Godin, J. G. J. 1986 Risk of predation and foraging behavior in shoaling banded killifish (*Fundulus diaphanus*). *Can. J. Zool.-Rev. Can. Zool.* **64**, 1675–1678. (doi:10.1139/z86-251)
4 Herskin, J. & Steffensen, J. F. 1998 Energy savings in sea bass swimming in a school: measurements of tail beat frequency and oxygen consumption at different swimming speeds. *J. Fish. Biol.* **53**, 366–376. (doi:10.1006/jfbi.1998.0708)
5 Magurran, A. E. & Pitcher, T. J. 1987 Provenance, shoal size and the sociobiology of predator-evasion behavior in minnow shoals. *Proc. R. Soc. Lond. B* **229**, 439–465. (doi:10.1098/rspb.1987.0004)
6 Pyke, G. H. 1978 Are animals efficient harvesters? *Anim. Behav.* **26**, 241–250. (doi:10.1016/0003-3472(78)90024-6)
7 Wilson, D. S. & Sober, E. 1989 Reviving the superorganism. *J. Theor. Biol.* **136**, 337–356. (doi:10.1016/s0022-5193(89)80169-9)
8 Huth, A. & Wissel, C. 1992 The simulation of the movement of fish schools. *J. Theor. Biol.* **156**, 365–385. (doi:10.1016/s0022-5193(05)80681-2)
9 Pulliam, H. R. & Caraco, T. 1984 Living in groups: is there an optimal group size? In *Behavioural ecology. An evolutionary approach* (eds J. R. Krebs & N. B. Davies), pp. 122–147. Oxford, UK: Blackwell Science.
10 Domenici, P. & Batty, R. S. 1994 Escape maneuvers of schooling *Clupea harengus*. *J. Fish. Biol.* **45**, 97–110. (doi:10.1111/j.1095-8649.1994.tb01086.x)
11 Reebs, S. G. 2000 Can a minority of informed leaders determine the foraging movements of a fish shoal? *Anim. Behav.* **59**, 403–409. (doi:10.1006/anbe.1999.1314)
12 Sumpter, D. J. T. 2010 *Collective animal behavior*. Princeton, NJ: Princeton University Press.
13 Marras, S., Claireaux, G., McKenzie, D. J. & Nelson, J. A. 2010 Individual variation and repeatability in aerobic and anaerobic swimming performance of European sea bass, *Dicentrarchus labrax*. *J. Exp. Biol.* **213**, 26–32. (doi:10.1242/jeb.032136)
14 Marras, S., Killen, S. S., Claireaux, G., Domenici, P. & McKenzie, D. J. 2011 Behavioural and kinematic components of the fast-start escape response in fish: individual variation and temporal repeatability. *J. Exp. Biol.* **214**, 3102–3110. (doi:10.1242/jeb.056648)
15 Killen, S. S., Marras, S., Steffensen, J. F. & McKenzie, D. J. 2012 Aerobic capacity influences the spatial position of individuals within fish schools. *Proc. R. Soc. B* **279**, 357–364. (doi:10.1098/rspb.2011.1006)
16 Harcourt, J. L., Ang, T. Z., Sweetman, G., Johnstone, R. A. & Manica, A. 2009 Social feedback and the emergence of leaders and followers. *Curr. Biol.* **19**, 248–252. (doi:10.1016/j.cub.2008.12.051)
17 Takanishi, A., Aoki, T., Ito, M., Ohkawa, Y. & Yamaguchi, J. 1998 Interaction between creature and robot: development of an experiment system for rat and rat robot interaction. In *IEEE/RSJ Int. Conf. on Intelligent Robots and Systems*, Victoria, BC, Canada, 13–17 October 1998, vol. 3, pp. 1975–1980. (doi:10.1109/IROS.1998.724896)
18 Vaughan, R., Sumpter, N., Henderson, J., Frost, A. & Cameron, S. 2000 Experiments in automatic flock control. *Robot. Auton. Syst.* **31**, 109–117. (doi:10.1016/s0921-8890(99)00084-6)
19 Kubinyi, E., Miklosi, A., Kaplan, F., Gacsi, M., Topal, J. & Csanyi, V. 2004 Social behaviour of dogs encountering AIBO, an animal-like robot in a neutral and in a feeding situation. *Behav. Process.* **65**, 231–239. (doi:10.1016/j.beproc.2003.10.003)
20 Halloy, J. *et al.* 2007 Social integration of robots into groups of cockroaches to control self-organized choices. *Science* **318**, 1155–1158. (doi:10.1126/science.1144259)
21 Partan, S. R., Larco, C. P. & Owens, M. J. 2009 Wild tree squirrels respond with multisensory enhancement to conspecific robot alarm behaviour. *Anim. Behav.* **77**, 1127–1135. (doi:10.1016/j.anbehav.2008.12.029)
22 Faria, J. J., Dyer, J. R. G., Clement, R. O., Couzin, I. D., Holt, N., Ward, A. J. W., Waters, D. & Krause, J. 2010 A novel method for investigating the collective behaviour of fish: introducing 'Robofish'. *Behav. Ecol. Sociobiol.* **64**, 1211–1218. (doi:10.1007/s00265-010-0988-y)
23 Ward, A. J. W., Sumpter, D. J. T., Couzin, I. D., Hart, P. J. B. & Krause, J. 2008 Quorum decision-making facilitates information transfer in fish shoals. *Proc. Natl Acad. Sci. USA* **105**, 6948–6953. (doi:10.1073/pnas.0710344105)
24 Sumpter, D. J. T., Krause, J., James, R., Couzin, I. D. & Ward, A. J. W. 2008 Consensus decision-making by fish. *Curr. Biol.* **18**, 1773–1777. (doi:10.1016/j.cub.2008.09.064)
25 Yen, J. & Weissburg, M. 2007 Perspectives on biologically inspired design: introduction to the collected contributions. *Bioinspiration Biomim.* **2**. (doi:10.1088/1748-3182/2/4/e01)
26 Liao, J. C., Beal, D. N., Lauder, G. V. & Triantafyllou, M. S. 2003 Fish exploiting vortices decrease muscle activity. *Science* **302**, 1566–1569. (doi:10.1126/science.1088295)

27 Svendsen, J. C., Skov, J., Bildsoe, M. & Steffensen, J. F. 2003 Intra-school positional preference and reduced tail beat frequency in trailing positions in schooling roach under experimental conditions. *J. Fish. Biol.* **62**, 834–846. (doi:10.1046/j.1095-8649.2003.00068.x)

28 Hall, D. J., Werner, E. E., Gilliam, J. F., Mittelbach, G. G., Howard, D., Doner, C. G., Dickerman, J. A. & Stewart, A. J. 1979 Diel foraging behavior and prey selection in the golden shiner (*Notemigonus crysoleucas*). *J. Fish. Res. Board of Canada* **36**, 1029–1039. (doi:10.1139/f79-145)

29 Abaid, N., Kopman, V. & Porfiri, M. In press. The story of a Brooklyn outreach program on biomimetics, underwater robotics, and marine science for K-12 students. *IEEE Robot. Autom. Mag.*

30 Kopman, V. & Porfiri, M. 2011 A miniature and low-cost robotic fish for ethorobotics research and engineering education I: bioinspired design. In *ASME DSCC—Dynamic Systems and Control Conference*, pp. MoBT6.3. Arlington, VA, USA.

31 Kopman, V. & Porfiri, M. Submitted. Miniature biomimetic robotic-fish for ethorobotics research and K-12 education: design and propulsion characterization.

32 Videler, J. J. 1993 *Fish swimming*. London, UK: Chapman & Hall.

33 Peterson, S. D., Porfiri, M. & Rovardi, A. 2009 A particle image velocimetry study of vibrating ionic polymer metal composites in aqueous environments. *IEEE/ASME Trans. Mechatron.* **14**, 474–483. (doi:10.1109/tmech.2009.2020979)

34 Adrian, R. J. & Westerweel, J. 2010 *Particle image velocimetry*. Cambridge, UK: Cambridge University Press.

35 Raffel, M., Willert, C. & Kompenhans, J. 1998 *Particle image velocimetry: a practical guide*. New York, NY: Springer.

36 Epps, B. P., Alvarado, P. V. Y., Youcef-Toumi, K. & Techet, A. H. 2009 Swimming performance of a biomimetic compliant fish-like robot. *Exp. Fluids* **6**, 927–939. (doi:10.1007/s00348-009-0684-8)

37 Sumner, D. 2010 Two circular cylinders in cross-flow: a review. *J. Fluids Struct.* **26**, 849–899. (doi:10.1016/j.jfluidstructs.2010.07.001)

38 Bachelet, E. 1981 *Circular statistics in biology*. London, UK: Academic Press.

39 Abdelnour, K., Mancia, E., Peterson, S. D. & Porfiri, M. 2009 Hydrodynamics of underwater propulsors based on ionic polymer-metal composites: a numerical study. *Smart Mater. Struct.* **18**, 085006. (doi:10.1088/0964-1726/18/8/085006)

40 Aureli, M., Kopman, V. & Porfiri, M. 2010 Free-locomotion of underwater vehicles actuated by ionic polymer metal composites. *IEEE/ASME Trans. Mechatron.* **15**, 603–614. (doi:10.1109/TMECH.2009.2030887)

41 Liu, F., Lee, K.-M. & Yang, C.-J. In press. Hydrodynamics of an undulating fin for a wave-like locomotion system design. *IEEE/ASME Trans. Mechatron.* (doi:10.1109/TMECH.2011.2107747)

42 Chen, Z., Sharata, S. & Tan, X. 2010 Modeling of biomimetic robotic fish propelled by an ionic polymer metal composite caudal fin. *IEEE/ASME Trans. Mechatron.* **15**, 448–459. (doi:10.1109/TMECH.2009.2027812)

43 Zar, J. 1984 *Biostatistical analysis*. Englewood Cliff, NJ: Prentice Hall.

44 Leblond, C. & Reebs, S. G. 2006 Individual leadership and boldness in shoals of golden shiners (*Notemigonus crysoleucas*). *Behaviour* **143**, 1263–1280. (doi:10.1163/156853906778691603)

45 Kiflawi, M. & Mazeroll, A. I. 2006 Female leadership during migration and the potential for sex-specific benefits of mass spawning in the brown surgeonfish (*Acanthurus nigrofuscus*). *Environ. Biol. Fishes* **76**, 19–23. (doi:10.1007/s10641-006-9003-x)

46 Nauen, J. C. & Lauder, G. V. 2002 Hydrodynamics of caudal fin locomotion by chub mackerel, *Scomber japonicus* (*Scombridae*). *J. Exp. Biol.* **205**, 1709–1724.

47 Lauder, G. V. & Tytell, E. D. 2006 Hydrodynamics of undulatory propulsion. In *Fish biomechanics* (ed. R. E. Shadwick & G. V. Lauder), vol. 23, pp. 425–468. San Diego, CA: Academic Press.

48 Taguchi, M. & Liao, J. C. 2011 Rainbow trout consume less oxygen in turbulence: the energetic of swimming behaviors at different speeds. *J. Exp. Biol.* **214**, 1428–1436. (doi:10.1242/jeb.052027)

49 Weihs, D. 1973 Hydromechanics of fish schooling. *Nature* **241**, 290–291. (doi:10.1038/241290a0)

50 Krause, J. 1993 The relationship between foraging and shoal position in a mixed shoal of roach (*Rutilus rutilus*) and chub (*Leuciscus cephalus*): a field study. *Oecologia* **93**, 356–359. (doi:10.1007/bf00317878)

51 DeBlois, E. M. & Rose, G. A. 1996 Cross-shoal variability in the feeding habits of migrating Atlantic cod (*Gadus morhua*). *Oecologia* (*Berl*) **108**, 192–196. (doi:10.1007/bf00333231)

52 Reebs, S. G. 2001 Influence of body size on leadership in shoals of golden shiners, *Notemigonus crysoleucas*. *Behaviour* **138**, 797–809. (doi:10.1163/156853901753172656)

53 Al-Imari, L. & Gerlai, R. 2008 Sight of conspecifics as reward in associative learning in zebrafish (*Danio rerio*). *Behav. Brain Res.* **189**, 216–219. (doi:10.1016/j.bbr.2007.12.007)